

---

# New kernel-based change-point detection

---

**Hoseung Song**

Public Health Sciences Division  
Fred Hutchinson Cancer Research Center  
Seattle, Washington 98109  
hsong3@fredhutch.org

**Hao Chen**

Department of Statistics  
University of California, Davis  
Davis, California 95616  
hxchen@ucdavis.edu

## Abstract

Change-point analysis plays a significant role in various fields to reveal discrepancies in distribution in a sequence of observations. While a number of algorithms have been proposed for high-dimensional data, kernel-based methods have not been well explored due to difficulties in controlling false discoveries and mediocre performance. In this paper, we propose a new kernel-based framework that makes use of an important pattern of data in high dimensions to boost power. Analytic approximations to the significance of the new statistics are derived and fast tests based on the asymptotic results are proposed, offering easy off-the-shelf tools for large datasets. The new tests show superior performance for a wide range of alternatives when compared with other state-of-the-art methods. We illustrate these new approaches through an analysis of a phone-call network data.

## 1 Introduction

Recent technological advances have facilitated the collection of high-dimensional data sequences in various high-impact applications, including social sciences [15, 27], neuroscience [23, 28], and computer graphics [20, 24]. High-dimensional complex data sequences are becoming prevalent and the development of efficient change-point detection method for them is gaining more and more attention. In this paper, we consider the offline change-point detection problem where a sequence of independent observations  $\{y_i\}_{1,\dots,n}$ ,  $y_i \in \mathcal{R}^d$ , is given at the time when data analysis is conducted. Specifically, we consider testing the null hypothesis

$$H_0 : y_i \sim F_0, i = 1, \dots, n \quad (1)$$

against the single change-point alternative

$$H_1 : \exists 1 \leq \tau < n, y_i \sim \begin{cases} F_0, & i \leq \tau \\ F_1, & \text{otherwise} \end{cases} \quad (2)$$

or the changed interval alternative

$$H_2 : \exists 1 \leq \tau_1 < \tau_2 < n, y_i \sim \begin{cases} F_0, & i = \tau_1 + 1, \dots, \tau_2 \\ F_1, & \text{otherwise} \end{cases} \quad (3)$$

where  $F_0$  and  $F_1$  are two different distributions.

A number of parametric approaches have been proposed, such as the methods in [5, 25, 26, 30]. However, parametric approaches for high-dimensional data in general impose strong assumptions – data shall follow or close to the particular parametric model. To overcome this, a few nonparametric approaches have been studied, such as the methods using marginal rankings [18], interpoint distances [16, 19], similarity graphs [4, 6], and Fréchet mean and variance [7].

## 1.1 Kernel change-point detection methods and their limitations

Kernel methods are useful tools under the two-sample hypothesis testing setting for high-dimensional data and they have the potential to capture any types of differences in the distribution. The most well-known method is the maximum mean discrepancy (MMD) test proposed by [9] where observations are mapped into a reproducing kernel Hilbert space (RKHS) generated by a given kernel  $k(\cdot, \cdot)$ . Compared with kernel methods in the two-sample testing setting, kernel-based change-point analysis received less attention.

The first practical offline change-point detection method using kernels was proposed by [11]. They incorporated kernels into dynamic programming algorithms. A kernel-based test statistic, called the maximum kernel Fisher discriminant ratio, was also proposed by [12]. However, the test statistic has  $O(n^3d)$  time complexity and the approach relies on the bootstrap resampling method for computing the decision threshold, making the test impractical in reality. [17] proposed MMD-based test statistic by adopting a strategy developed by [29]. Though it is computationally efficient when the amount of data is large, the method does not provide an estimate of the change-point (they provide an estimate of a block of the fixed length that contains the change-point) and requires a large amount of reference data before the change happens. Some other kernel-based methods were proposed [2, 13], but they do not provide an estimate of the location of change-points when the null hypothesis  $H_0$  (1) is rejected. Recently, [1] developed a kernel change-point detection procedure (KCP) that extends the method in [11]. KCP utilizes a model-selection penalty that allows to select the number of change-points, while the work of [11] assumes a fixed known number of change-points. However, it does not work well under some important types of changes due to the curse of dimensionality (see Section 2 for explanations and Section 4, Table 3 for its performance). Also, KCP heavily depends on the penalty constant and it is very difficult to control the type I error. Table 1 shows the empirical size of KCP under different dimensions and penalty constants for Gaussian data when  $n = 200$ . We see that the empirical size of the test is sensitive to the penalty constant, particularly for high-dimensional data.

Table 1: Empirical size of KCP under different dimensions and penalty constants for Gaussian data

	$d = 100$			$d = 500$			$d = 1000$		
Penalty constant	0.345	0.340	0.335	0.0590	0.0585	0.0580	0.0287	0.0282	0.0277
Empirical size	0.041	0.056	0.084	0.028	0.051	0.081	0.009	0.036	0.159

## 1.2 Our contribution

To the best of our knowledge, all existing kernel change-point detection methods are restricted to specific settings and miss some important types of changes. We propose new kernel-based test statistics that perform well for a wide range of alternatives and achieves high power in detecting and estimating change-points in the high-dimensional sequence compared to other state-of-the-art change-point detection methods. The new methods are easy to implement and have no tuning parameter. We also propose fast tests and derive analytic formulas for type I error control, allowing instant application to large datasets.

## 2 New scan statistics

In this section, the new scan statistics for testing the null  $H_0$  (1) against the single change-point alternative  $H_1$  (2) are presented and all materials for the changed-interval alternative  $H_2$  (3) are provided in Appendix G. We work under the permutation null distribution, which places  $1/n!$  probability on each of the  $n!$  permutations of  $\{y_i\}_{1,\dots,n}$ . We use  $\mathbf{P}_p$ ,  $\mathbf{E}_p$ ,  $\mathbf{Var}_p$ , and  $\mathbf{Cov}_p$  to denote the probability, expectation, variance, and covariance, respectively, under the permutation null distribution. In addition, without further specification, we use the Gaussian kernel with the median heuristic, the median of all pairwise distances among observations, as the bandwidth parameter.

In the above mentioned kernel change-point methods [1, 11, 13, 17], the MMD-based test statistic was used for constructing the scan statistics. MMD-based tests was proved to be consistent against all alternatives for the two-sample testing [10]. However, it could have very low power under finite sample sizes, such as in hundreds or thousands, for some common alternatives [22]. The

same problem also occurs under the change-point setting. For example, we consider Gaussian data  $N_d(\mathbf{0}_d, \Sigma)$  vs  $N_d(\mu\mathbf{1}_d, \sigma^2\Sigma)$  where  $n = 200$ ,  $\tau = 150$ ,  $\Sigma_{i,j} = 0.4^{|i-j|}$ ,  $\mathbf{0}_d$  and  $\mathbf{1}_d$  are  $d$  dimensional vectors of zeros, and ones, respectively, and  $d = 50$ . Based on an unbiased estimator of  $\text{MMD}^2$  [9], its scan statistic can be computed as

$$\begin{aligned} \text{MMD}_u^2(t) &= \frac{1}{t(t-1)} \sum_{i=1}^t \sum_{j=1, j \neq i}^t k(y_i, y_j) + \frac{1}{(n-t)(n-t-1)} \sum_{i=t+1}^n \sum_{j=t+1, j \neq i}^n k(y_i, y_j) \\ &\quad - \frac{2}{t(n-t)} \sum_{i=1}^t \sum_{j=t+1}^n k(y_i, y_j) \\ &\triangleq \alpha(t) + \beta(t) - 2\gamma(t) = \{\alpha(t) - \gamma(t)\} + \{\beta(t) - \gamma(t)\}. \end{aligned}$$

Figure 1 shows heatmaps of kernel matrices under different cases and the estimated power of  $\max_{n_0 \leq t \leq n_1} \text{MMD}_u^2(t)$  where  $n_0 = 0.05n$  and  $n_1 = n - n_0$  by 100 trials based on 10,000 bootstrap replicates. Under location changes (left panel), since kernel values are proportional to the similarity between two observations, we would expect both  $\alpha(t)$  and  $\beta(t)$  to be larger than  $\gamma(t)$ , which leads to large  $\text{MMD}_u^2(t)$  and high power. However, when there are additional variance changes (middle panel), due to the curses of dimensionality, samples from the distribution with a larger variance could be closer to samples from the distribution with a smaller variance (see more discussions on this phenomenon in [3]). Then the effects of  $\alpha(t) - \gamma(t)$  and  $\beta(t) - \gamma(t)$  could offset, which results in lower power with additional variance change on top of the mean change.

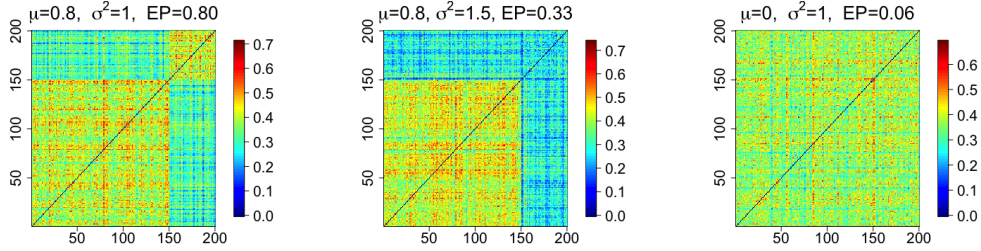


Figure 1: Heatmaps of kernel matrices under different cases and the estimated power of  $\max_{n_0 \leq t \leq n_1} \text{MMD}_u^2(t)$  (denoted by ‘EP’ in the title).

Let  $g_i(t) = I_{i>t}$ , where  $I_A$  is an indicator function that takes value 1 if  $A$  is true and 0 otherwise, and  $k_{ij} = k(y_i, y_j)$  ( $i, j = 1, \dots, n$ ). The quantity of  $\alpha$ ,  $\beta$  in testing the two samples  $\{y_1, \dots, y_t\}$  and  $\{y_{t+1}, \dots, y_n\}$  can be written as  $\alpha(t) = \frac{1}{t(t-1)} \sum_{i=1}^t \sum_{j=1, j \neq i}^t k_{ij} I_{g_i(t)=g_j(t)=0}$ ,  $\beta(t) = \frac{1}{(n-t)(n-t-1)} \sum_{i=1}^n \sum_{j=1, j \neq i}^n k_{ij} I_{g_i(t)=g_j(t)=1}$ . Based on the motivation, we define a scan statistic to aggregate deviations of  $\alpha(t)$  and  $\beta(t)$  from their expectations under the permutation null in both directions:

$$\text{GKCP}(t) = (\alpha(t) - \mathbb{E}_p(\alpha(t)), \beta(t) - \mathbb{E}_p(\beta(t))) \Sigma_t^{-1} \begin{pmatrix} \alpha(t) - \mathbb{E}_p(\alpha(t)) \\ \beta(t) - \mathbb{E}_p(\beta(t)) \end{pmatrix}, \quad (4)$$

where  $\Sigma_t = \text{Var}_p((\alpha(t), \beta(t))^T)$ . Under the permutation null, the analytic expressions for the expectation and the variance of  $\alpha(t)$  and  $\beta(t)$  can be calculated through combinatorial analysis. They are provided in Lemma 2.1 (proof in Appendix A.1).

**Lemma 2.1** *Under the permutation null, we have*

$$\begin{aligned} \mathbb{E}_p(\alpha(t)) &= \mathbb{E}_p(\beta(t)) = \frac{1}{n(n-1)} R_0 \triangleq \bar{k}, \\ \text{Var}_p(\alpha(t)) &= \frac{1}{t^2(t-1)^2} (2R_1 p_1(t) + 4R_2 p_2(t) + R_3 p_3(t)) - \bar{k}^2, \\ \text{Var}_p(\beta(t)) &= \frac{1}{(n-t)^2(n-t-1)^2} (2R_1 q_1(t) + 4R_2 q_2(t) + R_3 q_3(t)) - \bar{k}^2, \\ \text{Cov}_p(\alpha(t), \beta(t)) &= \frac{R_3}{n(n-1)(n-2)(n-3)} - \bar{k}^2, \end{aligned}$$

where

$$\begin{aligned}
R_0 &= \sum_{i=1}^n \sum_{j=1, j \neq i}^n k_{ij}, & R_1 &= \sum_{i=1}^n \sum_{j=1, j \neq i}^n k_{ij}^2, & R_2 &= \sum_{i=1}^n \sum_{j=1, j \neq i}^n \sum_{u=1, u \neq j, u \neq i}^n k_{ij} k_{iu}, \\
R_3 &= \sum_{i=1}^n \sum_{j=1, j \neq i}^n \sum_{u=1, u \neq j, u \neq i}^n \sum_{v=1, v \neq u, v \neq j, v \neq i}^n k_{ij} k_{uv}, \\
p_1(t) &= \frac{t(t-1)}{n(n-1)}, & p_2(t) &= p_1(t) \frac{t-2}{n-2}, & p_3(t) &= p_2(t) \frac{t-3}{n-3}, \\
q_1(t) &= \frac{(n-t)(n-t-1)}{n(n-1)}, & q_2(t) &= q_1(t) \frac{n-t-2}{n-2}, & q_3(t) &= q_2(t) \frac{n-t-3}{n-3}.
\end{aligned}$$

To test  $H_0$  (1) versus  $H_1$  (2), the following scan statistic is used:

$$\max_{n_0 \leq t \leq n_1} \text{GKCP}(t), \quad (5)$$

where  $n_0$  and  $n_1$  are pre-specified constraints on the region where the change-point  $\tau$  is searched. By default, we can set  $n_0 = \lceil 0.05n \rceil$  and  $n_1 = n - n_0$ . If there are prior information on the range of the potential change-point, then  $n_0$  and  $n_1$  can be specified accordingly. The null hypothesis  $H_0$  (1) is rejected if the scan statistic is greater than a threshold. Explorations on how to choose the threshold to control the type I error are discussed in Section 3.

**Remark 2.1** *When the length of sequence  $n$  is large, computing the whole kernel matrix might be computationally expensive. The block approach can be used to reduce the computation time [17], but this could lead to the performance trade-off due to loss of information.*

### 3 Faster tests with analytical $p$ -value approximations

Given the test statistic, the next step is to determine how large the test statistic needs to provide sufficient evidence to reject the null hypothesis of homogeneity. That is, we are concerned with the tail probabilities of the scan statistic under  $H_0$  (1),  $\mathbf{P}_p(\max_{n_0 \leq t \leq n_1} \text{GKCP}(t) > b)$ . The threshold can be approximated by drawing random permutations of the sequence. This is time consuming. We thus investigate the stochastic process to see if there is any way to make the test faster.

From the result in [22], it can be shown that

$$\text{GKCP}(t) = Z_D^2(t) + Z_W^2(t), \quad (6)$$

where

$$Z_D(t) = \frac{D(t) - \mathbf{E}_p(D(t))}{\sqrt{\text{Var}_p(D(t))}}, \quad Z_W(t) = \frac{W(t) - \mathbf{E}_p(W(t))}{\sqrt{\text{Var}_p(W(t))}} \quad (7)$$

with  $D(t) = t(t-1)\alpha(t) - (n-t)(n-t-1)\beta(t)$ ,  $W(t) = \frac{n-t}{n}\alpha(t) + \frac{t}{n}\beta(t)$ . [22] showed that the test of the two-sample version of  $Z_W(t)$  is equivalent to the test based on  $\text{MMD}_u^2$ , but the limiting distribution of  $\text{MMD}_u^2$  is not easy to handle [9]. Due to the intrinsic relation between the test based on  $\text{MMD}_u^2$  and  $W(t)$ , it is also not easy to handle the limiting distribution of  $W(t)$ . Hence, we first define a related quantity, an weighted version of  $W(t)$ , to obtain the tractable asymptotic results:

$$W_r(t) = r \frac{n-t}{n} t(t-1)\alpha(t) + \frac{t}{n} (n-t)(n-t-1)\beta(t). \quad (8)$$

$Z_{W,r}(t)$  is the standardized  $W_r(t)$ , where  $r$  is a constant.

#### 3.1 Asymptotic distributions of the basic processes

In this section, we derive the limiting distributions of  $\{Z_D([nu]) : 0 < u < 1\}$  and  $\{Z_{W,r}([nu]) : 0 < u < 1\}$ . In the following, we write  $a_n = O(b_n)$  when  $a_n$  has the same order as  $b_n$  and  $a_n = o(b_n)$  when  $a_n$  is dominated by  $b_n$  asymptotically, i.e.,  $\lim_{n \rightarrow \infty} (a_n/b_n) = 0$ . Let  $\tilde{k}_{ij} = (k_{ij} - \bar{k})I_{i \neq j}$  and  $\tilde{k}_{i\cdot} = \sum_{j=1, j \neq i}^n \tilde{k}_{ij}$  for  $i = 1, \dots, n$ . We work under the following two conditions.

<sup>1</sup> $[x]$  denotes the largest integer that is no larger than  $x$ .

**Condition 3.1**  $\sum_{i=1}^n |\tilde{k}_i|^s = o\left(\left\{\sum_{i=1}^n \tilde{k}_i^2\right\}^{s/2}\right)$  for all integers  $s > 2$ .

**Condition 3.2**  $\sum_{i=1}^n \sum_{j=1, j \neq i}^n \tilde{k}_{ij}^2 = o\left(\sum_{i=1}^n \tilde{k}_i^2\right)$ .

**Theorem 3.3** Under Condition 3.1 and 3.2, as  $n \rightarrow \infty$ ,

1.  $\{Z_D([nu]) : 0 < u < 1\}$  converges to a Gaussian process in finite dimensional distributions, which we denote as  $\{Z_D^*(u) : 0 < u < 1\}$ .
2.  $\{Z_{W,r}([nu]) : 0 < u < 1\}$  converges to a Gaussian process in finite dimensional distributions when  $r \neq 1$ , which we denote as  $\{Z_{W,r}^*(u) : 0 < u < 1\}$ .

The proof for this theorem is in Appendix A.2.

**Remark 3.4** Condition 3.1 can be satisfied when  $|\tilde{k}_i| = O(n^\delta)$  for a constant  $\delta, \forall i$ , and Condition 3.2 would further be satisfied if we also have  $\tilde{k}_{ij} = O(n^\kappa)$  for a constant  $\kappa < \delta - 0.5, \forall i, j$ . When there is no big outlier in the data, it is not hard to have all these conditions satisfied when one uses the Gaussian kernel with the median heuristic.

Let  $\rho_D^*(u, v) = \text{Cov}_p(Z_D^*(u), Z_D^*(v))$  and  $\rho_{W,r}^*(u, v) = \text{Cov}_p(Z_{W,r}^*(u), Z_{W,r}^*(v))$ . The explicit covariance functions of the limiting Gaussian processes,  $\{Z_D^*(u) : 0 < u < 1\}$  and  $\{Z_{W,r}^*(u) : 0 < u < 1\}$  are stated in the following theorem.

**Theorem 3.5** The exact expression for  $\rho_D^*(u, v)$  and  $\rho_{W,r}^*(u, v)$  are

$$\begin{aligned} \rho_D^*(u, v) &= \frac{(u \wedge v)(1 - (u \vee v))}{\sqrt{u(1-u)v(1-v)}}, \\ \rho_{W,r}^*(u, v) &= \frac{2R_1\{r^2(u \wedge v)(1 - (u \wedge v))(1 - (u \vee v)^2)\}}{(u \vee v)(1 - (u \wedge v))\sigma_{W,r}^*(u)\sigma_{W,r}^*(v)} \\ &\quad + \frac{2R_1\{r((u \vee v) - 1)(3uv - (u \wedge v)^2(2(u \vee v) + 1)) + uv(2 - (u \wedge v))(1 - (u \vee v))\}}{(u \vee v)(1 - (u \wedge v))\sigma_{W,r}^*(u)\sigma_{W,r}^*(v)} \\ &\quad + \frac{4R_2uv(1-u)(1-v)(r-1)^2}{(u \vee v)(1 - (u \wedge v))\sigma_{W,r}^*(u)\sigma_{W,r}^*(v)}, \end{aligned}$$

where  $u \wedge v = \min(u, v)$ ,  $u \vee v = \max(u, v)$ , and

$$\sigma_{W,r}^*(u) = \sqrt{2R_1\{r(1-u) + u\}^2 + (4R_1 + 4R_2)u(1-u)(r-1)^2}.$$

The above theorem is proved through combinatorial analysis and the details are in Appendix A.3. From the above theorem, we see that the limiting process  $\{Z_D^*(u) : 0 < u < 1\}$  does not depend on kernel values, while  $\{Z_{W,r}^*(u) : 0 < u < 1\}$ ,  $r \neq 1$ , depends on kernel values.

### 3.2 Asymptotic $p$ -value approximations

We now examine the asymptotic the behavior of tail probabilities. Following similar arguments in the proof for Proposition 3.4 in [4], when  $n_0, n_1, n, b \rightarrow \infty$  in a way such that for some  $0 < x_0 < x_1 < 1$  and  $b_0 > 0$ ,  $n_0/n \rightarrow x_0$ ,  $n_1/n \rightarrow x_1$ , and  $b/\sqrt{n} \rightarrow b_0$ , as  $n \rightarrow \infty$ , we have

$$\mathbb{P}_p\left(\max_{n_0 \leq t \leq n_1} |Z_D^*(t/n)| > b\right) \sim 2b\phi(b) \int_{x_0}^{x_1} h_D^*(x) \nu\left(b_0 \sqrt{2h_D^*(x)}\right) dx, \quad (9)$$

$$\mathbb{P}_p\left(\max_{n_0 \leq t \leq n_1} Z_{W,r}^*(t/n) > b\right) \sim b\phi(b) \int_{x_0}^{x_1} h_{W,r}^*(x) \nu\left(b_0 \sqrt{2h_{W,r}^*(x)}\right) dx, \quad (10)$$

where  $\nu(s) = (2/s)(\Phi(s/2) - 0.5) / ((s/2)\Phi(s/2) + \phi(s/2))$  [21] with  $\Phi(\cdot)$  and  $\phi(\cdot)$  being the standard normal cumulative density function and probability density function, respectively, and

$$h_D^*(x) = \lim_{s \nearrow x} \frac{\partial \rho_D^*(s, x)}{\partial s} = - \lim_{s \searrow x} \frac{\partial \rho_D^*(s, x)}{\partial s}, \quad h_{W,r}^*(x) = \lim_{s \nearrow x} \frac{\partial \rho_{W,r}^*(s, x)}{\partial s} = - \lim_{s \searrow x} \frac{\partial \rho_{W,r}^*(s, x)}{\partial s}.$$

**Remark 3.6** In practice, when using (9) and (10) for finite sample, we use

$$P_p \left( \max_{n_0 \leq t \leq n_1} |Z_D(t)| > b \right) \sim 2b\phi(b) \sum_{n_0 \leq t \leq n_1} C_D(t) \nu \left( b\sqrt{2C_D(t)} \right),$$

$$P_p \left( \max_{n_0 \leq t \leq n_1} Z_{W,r}(t) > b \right) \sim b\phi(b) \sum_{n_0 \leq t \leq n_1} C_{W,r}(t) \nu \left( b\sqrt{2C_{W,r}(t)} \right),$$

where

$$C_D(t) = \left. \frac{\partial \rho_D(s, t)}{\partial s} \right|_{s=t}, \quad C_{W,r}(t) = \left. \frac{\partial \rho_{W,r}(s, t)}{\partial s} \right|_{s=t}$$

with  $\rho_D(u, v) = \text{Cov}_p(Z_D(u), Z_D(v))$  and  $\rho_{W,r}(u, v) = \text{Cov}_p(Z_{W,r}(u), Z_{W,r}(v))$ . The explicit expressions for  $C_D(t)$  and  $C_{W,r}(t)$  can be calculated in the similar manner to the proof of Theorem 3.5 and provided in Appendix A.3.

### 3.3 Skewness correction

The analytical  $p$ -value approximations based on the asymptotic results provide a practical tool for large datasets. However, they become less precise if we set  $n_0$  and  $n_1$  close to the two ends since the convergence of  $Z_D(t)$  and  $Z_{W,r}(t)$  to the Gaussian process is slow as  $t/n$  is close to 0 or 1. Hence, we improve the accuracy of the analytical  $p$ -value approximations for finite sample sizes by skewness correction. As the skewness depends on the value of  $t$ , we adopt a similar treatment discussed in [4] by adding an extra term in the analytic formulas to correct skewness.

After skewness correction, the analytical  $p$ -value approximations are

$$P_p \left( \max_{n_0 \leq t \leq n_1} |Z_D^*(t/n)| > b \right) \sim 2b\phi(b) \int_{x_0}^{x_1} S_D(x) h_D^*(x) \nu \left( b_0 \sqrt{2h_D^*(x)} \right) dx, \quad (11)$$

$$P_p \left( \max_{n_0 \leq t \leq n_1} Z_{W,r}^*(t/n) > b \right) \sim b\phi(b) \int_{x_0}^{x_1} S_{W,r}(x) h_{W,r}^*(x) \nu \left( b_0 \sqrt{2h_{W,r}^*(x)} \right) dx, \quad (12)$$

where

$$S_D(t) = \frac{\exp \left\{ \frac{1}{2} (b - \hat{\theta}_{b,D}(t))^2 + \frac{1}{6} \gamma_D(t) \hat{\theta}_{b,D}^3(t) \right\}}{\sqrt{1 + \gamma_D(t) \hat{\theta}_{b,D}(t)}}, \quad \hat{\theta}_{b,D}(t) = \frac{\sqrt{1 + 2\gamma_D(t)b} - 1}{\gamma_D(t)},$$

and  $\gamma_D(t) = E_p(Z_D^3(t))$ .  $S_{W,r}(t)$ ,  $\hat{\theta}_{b,W,r}(t)$ , and  $\gamma_{W,r}(t)$  are defined in the same way. To obtain  $\gamma_D(t)$  and  $\gamma_{W,r}(t)$ , we need to figure out  $E_p(D^3(t))$  and  $E_p(W_r^3(t))$ . The exact analytic expressions of  $E_p(D^3(t))$  and  $E_p(W_r^3(t))$  are complicated and they are provided in Appendix B. We check how the analytical  $p$ -value approximations work for finite samples and the results are provided in Appendix C.

**Remark 3.7** When the marginal distribution is highly left-skewed, the skewness is so small that  $1 + 2\gamma(t)b$  could be negative. Since this problem usually happens when  $t/n$  is close to 0 or 1, we apply a heuristic fix discussed in [4] by extrapolating  $\hat{\theta}_b(t)$ .

### 3.4 Fast tests

Although  $Z_{W,r}(t)$  ( $r \neq 1$ ) converges to the Gaussian process under mild conditions, the performance of the test decreases as  $r$  goes away from 1 for location alternatives. Table 2 shows the estimated power of  $Z_{W,r}(t)$  under various  $r$  for Gaussian data where the first 100 observations are generated from  $N_d(\mu_1, I_d)$  and the second 100 observations are generated from  $N_d(\mu_2, I_d)$  with  $\|\mu_1 - \mu_2\|_2 := \Delta$ . The significance level is set to be 0.05 and the  $p$ -values of each test are approximated by 10,000 permutations for fair comparison.

To make use of the asymptotic result of  $Z_{W,r}(t)$  and maximize the power of the test, we propose to use  $Z_{W,1.2}(t)$  and  $Z_{W,0.8}(t)$  together. The power of the test could be enhanced in some common scenarios by using both test statistics together as they cover different regions of alternatives and their

$r$ 's are far enough away from 1 so that the Gaussian approximation is reasonable while maintaining a good power.

We now define two fast tests based on the asymptotic results. Let  $p_D$ ,  $p_{W,1.2}$ , and  $p_{W,0.8}$  be the approximated  $p$ -values of the test that reject for large values of  $|Z_D(t)|$ ,  $Z_{W,1.2}(t)$ , and  $Z_{W,0.8}(t)$ , respectively.

- fGKCP<sub>1</sub>: rejects the null hypothesis of homogeneity if  $3 \min(p_D, p_{W,1.2}, p_{W,0.8})$  is less than the significance level.
- fGKCP<sub>2</sub>: rejects the null hypothesis of homogeneity if  $2 \min(p_{W,1.2}, p_{W,0.8})$  is less than the significance level.

It is expected that fGKCP<sub>1</sub> performs well for a wide range of alternatives, especially for scale alternatives due to  $Z_D(t)$  (reasoning goes back to Figure 1). Since  $Z_W(t)$  is sensitive to location alternatives, we expect fGKCP<sub>2</sub> to be powerful for location alternatives. Furthermore, according to the simulation results, it turns out that fGKCP<sub>2</sub> can also detect variance changes to some extent as  $r = 1.2, 0.8$  cover more types of alternatives than  $r = 1$ . When the null hypothesis is rejected based on fGKCP<sub>1</sub>, the location of change-point can be estimated by  $\max_{n_0 \leq t \leq n_1} \text{GKCP}(t)$  so that the effects of  $Z_D(t)$  and  $Z_W(t)$  are fully utilized. We also propose to adopt the same rule for fGKCP<sub>2</sub> since GKCP( $t$ ) covers a wider range of alternatives (see Appendix D). For the fast tests as long as  $\max_{n_0 \leq t \leq n_1} Z_D(t)$ ,  $\max_{n_0 \leq t \leq n_1} Z_{W,1.2}(t)$ , and  $\max_{n_0 \leq t \leq n_1} Z_{W,0.8}(t)$  are computed, the tests can be conducted instantly.

Table 2: Estimated power of  $Z_{W,r}(t)$

		Location Alternatives				
$d$	$\Delta$	10	30	50	70	100
		0.31	0.60	0.77	0.96	1.13
$r = 1.3$		0.13	0.16	0.21	0.24	0.31
$r = 1.2$		0.13	0.22	0.34	0.40	0.47
$r = 1.1$		0.11	0.33	0.46	0.67	0.72
$r = 1.0$		0.12	<b>0.43</b>	<b>0.56</b>	<b>0.80</b>	<b>0.88</b>
$r = 0.9$		0.11	0.34	0.45	0.66	0.80
$r = 0.8$		0.12	0.25	0.27	0.38	0.49
$r = 0.7$		0.11	0.14	0.16	0.20	0.26

**Remark 3.8** We adopt the Bonferroni procedure for the fast tests to combine the advantages of each test statistic. To improve the power of the tests, the Simes procedure might be used and this also controls type I error well empirically (see Appendix E).

## 4 Performance of the new tests

We examine the performance of the new tests under various simulation settings. Each data sequence in the simulation is of length  $n = 200$  with various dimensions  $d$ , where  $y_1, \dots, y_\tau \stackrel{iid}{\sim} F_0$  and  $y_{\tau+1}, \dots, y_n \stackrel{iid}{\sim} F_1$ . Here,  $\tau$  is the change-point. We consider the following settings:

- Multivariate Gaussian:  $F_0 \sim N_d(\mathbf{0}_d, \Sigma)$  vs.  $F_1 \sim N_d(a\mathbf{1}_d, \sigma^2\Sigma)$ , where  $\Delta = \|a\mathbf{1}_d\|_2$  and  $\Sigma_{i,j} = 0.4^{|i-j|}$ .
- Chi-square data:  $\Sigma^{1/2}u_1$  vs.  $(\sigma^2\Sigma)^{1/2}u_2 + a\mathbf{1}_d$ , where  $\Delta = \|a\mathbf{1}_d\|_2$  and  $u_1$  and  $u_2$  are length- $d$  vectors with each component i.i.d. from the  $\chi_3^2$  distribution, and  $\Sigma_{i,j} = 0.4^{|i-j|}$ .
- Multivariate log-normal data:  $F_0 \sim \exp(N_d(\mathbf{0}_d, \Sigma))$  vs.  $F_1 \sim \exp(N_d(a\mathbf{1}_d, \Sigma))$ , where  $\Delta = \|a\mathbf{1}_d\|_2$  and  $\Sigma_{i,j} = 0.4^{|i-j|}$ .

More simulation results are provided in Appendix F. We simulate 100 datasets to estimate the power of the tests and the significance level is set to be 0.05 for all tests. To examine the empirical size of the test, we simulate 1,000 datasets. We also examine the accuracy of the estimated change-point location and the count where the location of estimated change-point is within 20 from the true change-point is provided in parentheses when the null is rejected.

It is usually hard to offer false positive controls as well as the estimation of the location of change-points. We compare the results of the new tests with the recent feasible kernel-based method, KCP [1], which was implemented in R package `ecp` [14]. We also compare the new tests with other feasible nonparametric methods using interpoint distances (ECP) [19] and similarity graphs (GCP) [6], which

was implemented in R packages `eCP` and `gSeg`, respectively. Here, we approximate the  $p$ -value by 1,000 permutation for GKCP and ECP, and use the max-type method with 5-MST for GCP, following the suggestion in [4]. Lastly, we include the method using Fréchet means and variances (FCP) with the  $p$ -value approximated by 5,000 bootstrap replicates [7].

Table 3: The number of null rejection and correctly detected change-points (in parentheses) for the multivariate Gaussian (top), chi-square (middle), and multivariate log-normal data (bottom) with  $n = 200$  (the methods with 95% of the best power under each setting are in bold)

Gaussian		Mean Change ( $\tau$ at center)				Variance Change ( $\tau$ at center)			
$d$		100	500	1000	2000	100	500	1000	2000
$\Delta   \sigma^2$		1.20	1.90	2.40	3.13	1.07	1.04	1.03	1.03
fGKCP <sub>1</sub>		50 (43)	68 (62)	78 (76)	<b>96 (95)</b>	<b>46 (30)</b>	<b>68 (52)</b>	<b>79 (64)</b>	<b>93 (81)</b>
fGKCP <sub>2</sub>		58 (49)	73 (67)	84 (80)	<b>97 (96)</b>	40 (25)	58 (43)	68 (54)	85 (73)
GKCP		<b>75 (63)</b>	<b>88 (82)</b>	<b>95 (91)</b>	<b>99 (98)</b>	41 (27)	<b>67 (51)</b>	<b>79 (63)</b>	<b>93 (80)</b>
KCP		71 (61)	<b>85 (79)</b>	<b>93 (90)</b>	<b>98 (97)</b>	18 (2)	15 (3)	12 (2)	7 (1)
ECP		<b>76 (65)</b>	<b>89 (79)</b>	<b>96 (90)</b>	<b>99 (95)</b>	5 (2)	6 (2)	6 (2)	6 (2)
GCP		22 (9)	27 (14)	34 (20)	46 (32)	27 (11)	40 (21)	49 (27)	64 (41)
FCP		6 (1)	1 (0)	0 (0)	0 (0)	13 (5)	0 (0)	0 (0)	0 (0)

Chi-square		Mean Change ( $\tau$ at center)				Variance Change ( $\tau$ at center)			
$d$		100	500	1000	2000	100	500	1000	2000
$\Delta   \sigma^2$		2.60	4.24	5.69	8.04	1.23	1.11	1.10	1.09
fGKCP <sub>1</sub>		24 (16)	40 (35)	45 (43)	80 (79)	<b>78 (62)</b>	<b>76 (56)</b>	<b>95 (82)</b>	<b>99 (92)</b>
fGKCP <sub>2</sub>		29 (19)	46 (40)	63 (60)	87 (86)	<b>81 (64)</b>	<b>78 (57)</b>	<b>95 (83)</b>	<b>99 (92)</b>
GKCP		<b>51 (40)</b>	<b>74 (64)</b>	<b>94 (88)</b>	<b>99 (99)</b>	75 (60)	71 (53)	<b>92(80)</b>	<b>99 (92)</b>
KCP		4 (0)	4 (0)	4 (0)	3 (0)	9 (0)	14 (0)	13 (0)	27 (0)
ECP		<b>58 (45)</b>	<b>78 (66)</b>	<b>94 (87)</b>	<b>99 (96)</b>	59 (46)	30 (18)	37 (26)	48 (38)
GCP		22 (8)	26 (10)	32 (19)	54 (38)	27 (11)	29 (10)	44 (22)	63 (37)
FCP		5 (0)	2 (0)	0 (0)	0 (0)	53 (35)	6 (2)	2 (0)	0 (0)

Log-normal		Mean Change ( $\tau$ at center)				Mean Change ( $\tau$ at three quarter)			
$d$		100	500	1000	2000	100	500	1000	2000
$\Delta$		1.20	1.90	2.30	3.04	1.35	2.12	2.65	3.42
fGKCP <sub>1</sub>		47 (35)	70 (57)	81 (71)	<b>96 (90)</b>	47 (38)	67 (58)	83 (77)	<b>95 (92)</b>
fGKCP <sub>2</sub>		55 (41)	76 (63)	85 (75)	<b>97 (91)</b>	53 (43)	73 (63)	86 (80)	<b>97 (94)</b>
GKCP		63 (48)	<b>83 (68)</b>	<b>91 (80)</b>	<b>99 (93)</b>	<b>65 (53)</b>	<b>86 (75)</b>	<b>95 (88)</b>	<b>99 (96)</b>
KCP		20 (16)	6 (5)	10 (9)	5 (4)	20 (16)	5 (4)	12 (9)	7 (5)
ECP		<b>69 (52)</b>	<b>85 (72)</b>	<b>91 (80)</b>	<b>98 (91)</b>	<b>62 (54)</b>	81 (70)	90 (82)	<b>97 (90)</b>
GCP		32 (12)	33 (7)	32 (6)	36 (8)	17 (3)	12 (0)	10 (0)	12 (0)
FCP		32 (18)	57 (40)	69 (53)	83 (70)	36 (24)	55 (41)	66 (55)	77 (67)

Table 4: Empirical size of the tests at 0.05 significance level with  $n = 200$

$d$	Multivariate Gaussian				Multivariate log-normal			
	100	500	1000	2000	100	500	1000	2000
fGKCP <sub>1</sub>	0.032	0.047	0.047	0.037	0.038	0.039	0.041	0.036
fGKCP <sub>2</sub>	0.043	0.057	0.055	0.052	0.051	0.050	0.050	0.055
GKCP	0.052	0.049	0.053	0.049	0.049	0.051	0.038	0.056
KCP	0.067	0.045	0.060	0.040	0.093	0.040	0.081	0.067
ECP	0.054	0.043	0.056	0.045	0.054	0.057	0.051	0.042
GCP	0.072	0.073	0.069	0.077	0.090	0.132	0.098	0.113
FCP	0.018	0.001	0.000	0.000	0.053	0.051	0.036	0.027



Table 3 shows the number of rejection for the multivariate Gaussian, chi-square, and multivariate log-normal data with different means and/or variances. The count where the estimated change-point is within 20 from the true change-point is provided in parentheses when the null hypothesis is rejected. For the multivariate Gaussian data, we see that KCP and ECP perform well for location alternatives, while they have considerable low or no power for scale alternatives. On the other hand, the new test GKCP performs very well for both location and scale alternatives and the fast tests, fGKCP<sub>1</sub> and fGKCP<sub>2</sub>, also perform well. Other tests, GCP and FCP, do not work well for Gaussian settings. Alternatives in the multivariate log-normal data yield the changes in both the mean and variance of distributions. For the chi-square and multivariate log-normal data, we still see that the new tests in general outperform other tests and exhibit high power not only for symmetric distributions but also for asymmetric distributions under moderate to high dimensions.

The empirical size of the tests at 0.05 significance level for the multivariate Gaussian and log-normal data is presented in Table 4. We see that the new tests control the type I error rate well. However, KCP relies on a cumbersome method, such as the line search, to find the suitable penalty constant and this step is very sensitive, so it is difficult to control the type I error well.

The overall pattern of the simulation results shows that the new tests exhibit high power for a wide range of alternatives. Unlike the existing kernel change-point detection method, the new tests are effective and easy to implement without any time-consuming procedures, such as parameter tuning, as long as the kernel matrix is computed. In practice, fGKCP<sub>1</sub> and fGKCP<sub>2</sub> would be preferred as they are faster than GKCP. However, if the test result is ambiguous and further investigation is needed, such as  $p$ -value close to the nominal level, the permutation test of GKCP would also be useful.

## 5 A real data example

We apply the new tests to the phone-call network dataset. The MIT Media Laboratory studied 87 subjects who used mobile phones with a pre-installed device that can record call logs. The study lasted for 330 days from July 2004 to June 2005 [8]. This dataset can be requested from the MIT Reality Commons website (<http://realitycommons.media.mit.edu/realitymining.html>) and the personally identifiable information were not included in the dataset. We use it to illustrate the new tests by detecting any change in the phone-call pattern among subjects over time. This can be viewed as the change of friendship along time. We bin the phone-calls by day and we construct  $n = 330$  of networks in total with 87 subjects as nodes. We encode each network by the adjacency matrix with value 1 for element  $(i, j)$  if subject  $i$  called  $j$  on day  $t$  and 0 otherwise. We then construct the Gaussian kernel matrix with the median heuristic using the vectorized adjacency matrix. We apply the single change-point detection method to the phone-call network dataset recursively in order to detect all possible change-points. Since this dataset has a lot of noises, we focus on the estimated change-points with  $p$ -value less than 0.001.

Table 5: Estimated change-points and nearby academic events (the dates of the academic events are from the 2011-2012 academic calendar of MIT that is the closest academic calendar of MIT to 2004-2005 available online)

Estimated change-points	Nearby academic events
$t = 53$ : 2004/09/10	2004/09/07: Fall classes begin
$t = 90$ : 2004/10/17	2004/10/14: Family weekend
$t = 141$ : 2004/12/07	2004/12/14: Last day of Fall classes
$t = 251$ : 2005/03/27	2005/03/26: Spring break begins
$t = 293$ : 2005/05/08	2005/05/17: Last day of Spring classes

Table 5 shows the estimated change-points until the new tests do not reject the null. In this analysis, all new tests (GKCP, fGKCP<sub>1</sub>, fGKCP<sub>2</sub>) yield the same results about whether to reject the null or not in each iteration and the estimated locations of change-point. We also compare the results of the new tests with their nearby academic events. We see that the new tests detect change-points at around the beginning of the Fall term, family weekend, and the end of the Fall term that could cause phone-call pattern changes among subjects. The new tests also detect the Spring break and the end of the Spring term. These are all reasonable times when there are some significant changes in phone-call pattern.

## References

- [1] Sylvain Arlot, Alain Celisse, and Zaid Harchaoui. A kernel multiple change-point algorithm via model selection. *Journal of Machine Learning Research*, 20(162):1–56, 2019.
- [2] Wei-Cheng Chang, Chun-Liang Li, Yiming Yang, and Barnabás Póczos. Kernel change-point detection with auxiliary deep generative models. *arXiv preprint arXiv:1901.06077*, 2019.
- [3] Hao Chen and Jerome H Friedman. A new graph-based two-sample test for multivariate and object data. *Journal of the American statistical association*, 112(517):397–409, 2017.
- [4] Hao Chen and Nancy Zhang. Graph-based change-point detection. *The Annals of Statistics*, 43(1):139–176, 2015.
- [5] Jie Chen and Arjun K Gupta. *Parametric statistical change point analysis: with applications to genetics, medicine, and finance*. Springer Science & Business Media, 2011.
- [6] Lynna Chu and Hao Chen. Asymptotic distribution-free change-point detection for multivariate and non-euclidean data. *The Annals of Statistics*, 47(1):382–414, 2019.
- [7] Paromita Dubey and Hans-Georg Müller. Fréchet change-point detection. *Annals of Statistics*, 48(6):3312–3335, 2020.
- [8] Nathan Eagle, Alex Sandy Pentland, and David Lazer. Inferring friendship network structure by using mobile phone data. *Proceedings of the national academy of sciences*, 106(36):15274–15278, 2009.
- [9] Arthur Gretton, Karsten M Borgwardt, Malte Rasch, Bernhard Schölkopf, and Alex J Smola. A kernel method for the two-sample-problem. In *Advances in neural information processing systems*, pages 513–520, 2007.
- [10] Arthur Gretton et al. A kernel two-sample test. *Journal of Machine Learning Research*, 13(Mar):723–773, 2012.
- [11] Zaid Harchaoui and Olivier Cappé. Retrospective multiple change-point estimation with kernels. In *2007 IEEE/SP 14th Workshop on Statistical Signal Processing*, pages 768–772. IEEE, 2007.
- [12] Zaid Harchaoui, Eric Moulines, and Francis R Bach. Kernel change-point analysis. In *Advances in neural information processing systems*, pages 609–616, 2009.
- [13] Shuai Huang, Zhenyu Kong, and Wenzhen Huang. High-dimensional process monitoring and change point detection using embedding distributions in reproducing kernel hilbert space. *IIE Transactions*, 46(10):999–1016, 2014.
- [14] Nicholas A James and David S Matteson. ecp: An r package for nonparametric multiple change point analysis of multivariate data. *Journal of Statistical Software*, 62(7):1–25, 2015.
- [15] Lucy Kendrick, Katarzyna Musial, and Bogdan Gabrys. Change point detection in social networks—critical review with experiments. *Computer Science Review*, 29:1–13, 2018.
- [16] Jun Li. Asymptotic distribution-free change-point detection based on interpoint distances for high-dimensional data. *Journal of Nonparametric Statistics*, 32(1):157–184, 2020.
- [17] Shuang Li, Yao Xie, Hanjun Dai, and Le Song. M-statistic for kernel change-point detection. In *Advances in Neural Information Processing Systems*, pages 3366–3374, 2015.
- [18] Alexandre Lung-Yut-Fong, Céline Lévy-Leduc, and Olivier Cappé. Homogeneity and change-point detection tests for multivariate data using rank statistics. *Journal de la Société Française de Statistique*, 156(4):133–162, 2015.
- [19] David S Matteson and Nicholas A James. A nonparametric approach for multiple change point analysis of multivariate data. *Journal of the American Statistical Association*, 109(505):334–345, 2014.

- [20] Richard J Radke, Srinivas Andra, Omar Al-Kofahi, and Badrinath Roysam. Image change detection algorithms: a systematic survey. *IEEE transactions on image processing*, 14(3):294–307, 2005.
- [21] David Siegmund and Benjamin Yakir. *The statistics of gene mapping*. Springer Science & Business Media, 2007.
- [22] Hoseung Song and Hao Chen. Generalized kernel two-sample tests. *arXiv preprint arXiv:2011.06127*, 2020.
- [23] M Staudacher, S Telser, A Amann, H Hinterhuber, and M Ritsch-Marte. A new method for change-point detection developed for on-line analysis of the heart beat variability during sleep. *Physica A: Statistical Mechanics and its Applications*, 349(3-4):582–596, 2005.
- [24] Alexander G Tartakovsky, Aleksey S Polunchenko, and Grigory Sokolov. Efficient computer network anomaly detection by changepoint detection methods. *IEEE Journal of Selected Topics in Signal Processing*, 7(1):4–11, 2012.
- [25] Guanghai Wang, Changliang Zou, and Guosheng Yin. Change-point detection in multinomial data with a large number of categories. *Annals of Statistics*, 2017.
- [26] Tengyao Wang and Richard J Samworth. High dimensional change point estimation via sparse projection. *Journal of the Royal Statistical Society: Series B (Statistical Methodology)*, 80(1):57–83, 2018.
- [27] Yu Wang, Aniket Chakrabarti, David Sivakoff, and Srinivasan Parthasarathy. Fast change point detection on dynamic social networks. *arXiv preprint arXiv:1705.07325*, 2017.
- [28] Yuting Xu and Martin A Lindquist. Dynamic connectivity detection: an algorithm for determining functional connectivity change points in fmri data. *Frontiers in neuroscience*, 9:285, 2015.
- [29] Wojciech Zaremba, Arthur Gretton, and Matthew Blaschko. B-test: A non-parametric, low variance kernel two-sample test. In *Advances in neural information processing systems*, pages 755–763, 2013.
- [30] Nancy R Zhang, David O Siegmund, Hanlee Ji, and Jun Z Li. Detecting simultaneous change-points in multiple sequences. *Biometrika*, 2010.